Integral Equation Theory for Compressible Polymer Alloys: Thermodynamics, Scattering, and Miscibility of Gaussian Chains†

John G. Curro*

Sandia National Laboratories, Albuquerque, New Mexico 87185

Kenneth S. Schweizer

Department of Materials Science and Engineering, University of Illinois, Urbana, Illinois 61801

Received May 17, 1991

ABSTRACT: A series of numerical calculations are performed on binary mixtures of Gaussian chains using our recently developed integral equation theory of polymer blends. The intermolecular radial distribution function, structure factor, χ parameter, spinodal temperature, and compressibility are investigated over a range of molecular parameters. Structurally symmetric (the symmetric isotope blend) and various structurally asymmetric mixtures were studied. We find that the integral equation approach, which includes the effects of concentration fluctuations and nonrandom packing, leads to an increase in miscibility relative to the Flory–Huggins theory. For the symmetric isotope blend the χ parameter, calculated at fixed temperature and composition, decreases linearly with $N^{-1/2}$ for large degrees of polymerization N. Our calculations of χ as a function of composition for the symmetric isotopic blend are in good qualitative agreement with recent SANS measurements of Bates and co-workers. The wave vector dependence of the effective χ parameter is calculated and the implications with regard to block copolymers is discussed. The dependence of χ on temperature, composition, and N is systematically studied. We find that the incompressible random phase approximation (RPA) agrees with fully compressible calculations for the partial structure factors in the case of the symmetric isotope, but progressively deterioriates as structural asymmetry between the components is increased due to compressibility effects. Whereas the RPA predicts a large increase in miscibility as the disparity in segment lengths between the components increases, calculations of the critical temperature which include density fluctuations show only a relatively small enhancement. A striking result from this integral equation theory of polymer blends is that the upper critical solution temperature is proportional to $\sqrt{N}$ rather than a linear N dependence predicted by the Flory–Huggins theory. This unexpected molecular weight dependence, which is a consequence of the correlation hole, is found for both structurally symmetric and weakly asymmetric blends.

I. Introduction

The study of polymer blends continues to be an active area of research in polymer science. From an experimental standpoint, small-angle neutron scattering (SANS) has proven to be a powerful tool to study the thermodynamics and structure of polymer mixtures.[1] In recent years SANS measurements have shown behavior which was unexpected and in distinct contradiction to the well-known Flory–Huggins theory.[2] In particular, the Flory–Huggins χ parameter is not simply of the form χ = constant/T, but is found to depend on many other variables such as concentration, molecular weight, chemical and topological structure,[1,3-5] and even wave vector.[6] It is important to understand the origin of these nonclassical effects if one is to "molecularly engineer" new polymer blends of technological importance.

We have recently developed a novel integral equation theory for understanding the structure and thermodynamics of polymer liquids and melts.[7-11] This new approach for polymer liquids is based on the reference interaction site model (RISM theory) of Chandler and Andersen,[12,13] which has been very successful for small-molecule liquids. Our polymer integral equation theory ("polymer RISM" theory, not to be confused with "rotational isomeric state model") was found to be in very good agreement with the intermolecular radial distribution function from molecular dynamics simulations of homopolymer chains at liquidlike densities.[14,15] Excellent agreement of the theory was also found for the structure factor of polyethylene melts as measured by X-ray scattering.[16]

We have also extended our integral equation formalism to polymer blends.[17-20] For the case of a binary mixture, we are able to rigorously interpret the Flory–Huggins χ parameter in terms of direct correlation functions obtained by solving three coupled, integral equations. The solution of these integral equations, in general, requires numerical techniques. In some special cases, such as a symmetric isotope blend at 50/50 composition, and athermal mixtures at infinite molecular weight, we are able to obtain approximate analytical solutions.[21,22] In fact, using approximate analytical techniques, we are able to make some general predictions regarding the miscibility of polymer mixtures in various spatial dimensions and fractal architectures.[22]

Unfortunately, only a few cases are amenable to analytical treatment and even then only qualitative trends can be inferred. In order to make quantitative calculations on polymer mixtures numerical solution of the integral equations is required. The purpose of the present paper is to present the results of a series of systematic, numerical calculations on binary mixtures of Gaussian chains. In the next section we give a brief overview of our integral equation theory of blends. We also discuss in some detail the calculation of thermodynamic quantities. In particular we show how the isothermal compressibility and spinodal condition of a blend is related to the Fourier transform of the direct correlation functions evaluated at zero wave vector. With this theoretical background we then present results for the *symmetric isotope blend*, a binary mixture

† This work supported by the U.S. Department of Energy under Contract DE-AC0476DP00789.

0024-9297/91/2224-6736$02.50/0

of deuterated/hydrogenated chains of identical structure. In this case we find that the random phase approximation (RPA) theory of de Gennes[23] works well and we emphasize the dependence of the χ parameter on composition and molecular weight. We then discuss the consequences of breaking the structural symmetry between the components. Here we will demonstrate the limitations of the RPA formula due to compressibility effects and present results for the spinodal temperature as a function of molecular weight and extent of structural asymmetry. One of the important results that emerges from these studies is that the UCST spinodal temperature scales in a nonclassical way with the degree of polymerization, $T_s \propto \sqrt{N}$. This surprising result seems to hold for both symmetric and weakly asymmetric, compressible blends.

II. Theory

Our integral equation theory of polymer mixtures has been discussed in detail elsewhere.[19,20] Here we will present only the key results which are important for our present purposes. Following the RISM theory of Chandler and Andersen,[12,13] the polymer molecules are envisioned to consist of spherically symmetric sites. Interactions and correlations between polymer chains occur only between these sites. For the case of a binary blend of homopolymers for which chain end effects have been preaveraged, there are three independent *inter*molecular radial distribution functions $\{g_{AA}(r), g_{BB}(r), g_{AB}(r)\}$ representing correlations between intermolecular sites of like (AA or BB) and unlike (AB) species. The three corresponding intermolecular direct correlation functions $\{C_{AA}(r), C_{BB}(r), C_{AB}(r)\}$ are then defined through generalized Ornstein–Zernike-like matrix equations[12,13] given in Fourier space as

$$\hat{\mathbf{H}}(k) = \hat{\Omega}(k)\cdot\hat{\mathbf{C}}(k)\cdot[\hat{\Omega}(k) + \hat{\mathbf{H}}(k)] \tag{1}$$

where the caret denotes Fourier transformation and k is the wave vector. $\mathbf{C}(r)$ is the direct correlation function matrix and the matrices $\mathbf{H}(r)$ and $\Omega(r)$ are defined to be

$$H_{MM'}(r) = \rho_M\rho_{M'}[g_{MM'}(r) - 1]$$
$$\Omega_{MM'}(r) = \delta_{MM'}\rho_M\omega_M(r)$$

with ρ_M the site (monomer) density of species M = A or B. The polymer structural information enters the theory solely through the *intra*molecular distribution functions $\omega_A(r)$ and $\omega_B(r)$ defined according to

$$\omega_M(r) = N_M^{-1}\sum_{ij}^{N_M}\omega_{ij}(r;M) \tag{2}$$

where $\omega_{ij}(r;M)$ is the probability that a pair of sites i and j on the same chain (having N_M sites of type M) are separated by a distance r.

The direct correlation functions defined in eq 1 are generally believed to be spatially short range and play the role of renormalized pair potentials which account, in an average sense, for many-body structural effects. One then makes use of the approximate Percus–Yevick mean spherical closure.[12,17]

$$H_{MM'}(r) = -\rho_M\rho_{M'} \qquad r < d_{MM'}$$
$$C_{MM'}(r) \cong -v_{MM'}(r)/k_BT \qquad r > d_{MM'} \tag{3}$$

Equations 1 and 3 lead to three coupled, nonlinear integral equations for the three $g(r)$'s. The potential of interaction $v_{MM'}(r)$ between intermolecular sites is taken to be hard sphere with a superimposed Lennard-Jones attraction

$$v_{MM'}(r) = \begin{cases} \infty & r < d_{MM'} \\ \epsilon_{MM'}[(r/d_{MM'})^{-12} - 2(r/d_{MM'})^{-6}] & r \geq d_{MM'} \end{cases} \tag{4}$$

where M and M' are species indexes A or B, $\epsilon_{MM'}$ is the corresponding well depth, and $d_{MM'}$ is the hard-core diameter. For convenience we will take $d_{AB} = (d_{AA} + d_{BB})/2$.

In general, for flexible molecules the intramolecular structure in eq 2 and the intermolecular correlations are coupled together so that one needs to solve the integral equations self-consistently.[10,13] We have recently been able to perform this self-consistent calculation for the case of a homopolymer melt.[24] In the binary blend case considered here, we will follow our previous zeroth order approach and avoid the intramolecular/intermolecular self-consistency issue by assuming that the intramolecular structure of both components is ideal. This ideality conjecture of Flory[25] is well-known to be reasonably accurate in the homopolymer melt down to nearly monomeric length scales on the basis of neutron scattering and computer simulation studies. The ideality assumption is much more uncertain in mixtures, and it is possible to generalize our homopolymer self-consistent methods[24] to the blend and copolymer cases. Such calculations are beyond the scope of the present investigation and are reserved for future work on polymer systems with more realistic intrachain structure, which includes chain stiffness. In the present investigation we take $\omega_{ij}(r;M)$ to be a fully flexible Gaussian form for which eq 2 reduces to

$$\hat{\omega}_M(k) = (1 - f_M)^{-2}[1 - f_M^2 - 2N_M^{-1}f_M + 2N_M^{-1}f_M^{N_M+1}] \tag{5}$$

where

$$f_M = \exp(-k^2\sigma_M^2/6)$$

where σ_A and σ_B are the statistical segment length of each species. $\hat{\omega}_A(k)$ and $\hat{\omega}_B(k)$ are Fourier transforms of eq 2 and are defined to be the *intra*molecular structure factors of chains of type A or B.

We define the three partial structure factors $\hat{S}_{AA}(k)$, $\hat{S}_{BB}(k)$, and $\hat{S}_{AB}(k)$ in terms of the corresponding monomer density fluctuations $\delta\rho_M = \rho_M(r) - \rho_M$

$$\hat{S}_{MM'}(k) = \frac{1}{8\pi^3}\int d(\vec{r} - \vec{r}')\exp[i\vec{k}\cdot(\vec{r} - \vec{r}')]\langle\delta\rho_M(r)\delta\rho_{M'}(r')\rangle \tag{6a}$$

$$\hat{S}_{MM'}(k) = \rho_M\hat{\omega}_M(k)\delta_{MM'} + \rho_M\rho_{M'}\hat{h}_{MM'}(k) \tag{6b}$$

Using the generalized Ornstein–Zernike-like equations, it is possible to express these partial structure factors in terms of the three direct correlation functions

$$\hat{S}_{AA}(k) = \rho_A\hat{\omega}_A(1 - \rho_B\hat{\omega}_B\hat{C}_{BB})/\hat{\Lambda}$$
$$\hat{S}_{BB}(k) = \rho_B\hat{\omega}_B(1 - \rho_A\hat{\omega}_A\hat{C}_{AA})/\hat{\Lambda}$$
$$\hat{S}_{AB}(k) = \rho_A\rho_B\hat{\omega}_A\hat{\omega}_B\hat{C}_{AB}/\hat{\Lambda} \tag{7}$$

where the denominator contains terms nonlinear in the direct correlation functions and is given by

$$\hat{\Lambda}(k) = 1 - \rho_A\hat{\omega}_A\hat{C}_{AA} - \rho_B\hat{\omega}_B\hat{C}_{BB} + \rho_A\rho_B\hat{\omega}_A\hat{\omega}_B(\hat{C}_{AA}\hat{C}_{BB} - \hat{C}_{AB}^2) \tag{8}$$

Generalization of eqs 6–8 to treat copolymers is a trivial exercise in matrix algebra and requires only including an off-diagonal component of the $\hat{\Omega}(k)$ matrix in eq 1 that describes copolymer connectivity. It should be emphasized that in principle eqs 7 are exact and hence include *all* non-mean-field "fluctuation effects", both "critical-like" and "local". Equation 7 can be used to calculate the

structure factors once the direct correlation functions are known by solution of the three polymer RISM integral equations.

For a hypothetical incompressible system there is only one independent structure factor, which we call $\hat{S}_{RPA}(k)$.

$$\hat{S}_{RPA}(k) = K_{AA}\hat{S}_{AA}(k) = K_{BB}\hat{S}_{BB}(k) = -K_{AB}\hat{S}_{AB}(k)$$

where the normalization coefficients $K_{MM'}$ are defined to be[19,20]

$$K_{MM'} = \bar{v}_M\bar{v}_{M'}/\eta(\bar{v}_A\bar{v}_B)^{1/2} \qquad \eta = \rho_A\bar{v}_A + \rho_B\bar{v}_B$$

with η being the packing fraction and $\bar{v}_M$ the site or monomer volume of species A or B. In the special case of an incompressible system, we have shown previously[17,19] that we recover precisely the RPA form of de Gennes[23]

$$\frac{1}{\hat{S}_{RPA}(k)} = \frac{1}{R^{1/2}\phi\hat{\omega}_A(k)} + \frac{R^{1/2}}{(1-\phi)\hat{\omega}_B(k)} - 2\hat{\chi}_s(k) \quad (9)$$

where $R = \bar{v}_A/\bar{v}_B$ is the ratio of monomer volumes of the two species and $\phi = \rho_A\bar{v}_A/\eta$ is the volume fraction of component A. It must be emphasized that this formula assumes *only* zero compressibility. It is valid for arbitrary intramolecular structures, including cases where ideal single-chain statistics do not apply. $\chi_s(k)$ is a generalized χ parameter and is related to the Fourier transform of the direct correlation functions between like and unlike species

$$2\hat{\chi}_s(k) = \frac{\rho}{[R^{-1/2}\phi + R^{1/2}(1-\phi)]}[R^{-1}\hat{C}_{AA}(k) + R\hat{C}_{BB}(k) - 2\hat{C}_{AB}(k)] \quad (10)$$

where $\rho = \rho_A + \rho_B$. The $k \to 0$ limit of eq 10, χ_s, is analogous to the Flory–Huggins definition of χ except that the bare nearest-neighbor attractive interactions are now replaced by the corresponding direct correlation functions.

The analog of eqs 9 and 10 for diblock copolymers, consisting of N_A and N_B sequences of types A and B, respectively, is particularly simple. Using eq 1, neglecting chain end and copolymer junction effects on the direct correlation functions, and repeating precisely the same incompressible functional expansion analysis given previously for binary blends,[19] one can easily derive the result

$$\frac{1}{\hat{S}_{RPA}(k)} = \hat{F}(k) - 2\hat{\chi}_s(k)$$

$$\hat{F}(k) \equiv \frac{2[\hat{\omega}_A(k) + \hat{\omega}_B(k) + 2\hat{\omega}_{AB}(k)]}{[\hat{\omega}_A\hat{\omega}_B - \hat{\omega}_{AB}^2]}$$

For simplicity we have displayed only the $\phi = 0.5$, symmetric case ($N_A = N_B = n/2$) in which the monomer volumes are equal ($R = 1$). The intramolecular structure cross term, $\hat{\omega}_{AB}(k)$, which is zero in the blend case, is given by the Fourier transform of

$$\omega_{AB}(r) = 2n^{-1}\sum_{i\in A}\sum_{j\in B}\omega_{ij}(r;A,B)$$

where the probability $\omega_{ij}(r;A,B)$ that site i of type A is separated from site j of type B by a distance r is summed over i (A sites) and j (B sites). The above equation for $\hat{S}_{RPA}(k)$ is of the form of the RPA expression for block copolymers first derived by Leibler.[23] As noted for the blend case, it is far more general than the conditions associated with the standard derivation, since only incompressibility has been assumed and not any *weak segregation* restrictions. The single-chain partial structure factors $\hat{\omega}_A(k)$, $\hat{\omega}_B(k)$, and $\hat{\omega}_{AB}(k)$ are in general non-Gaussian and must be self-consistently determined with the *intermolecular* pair correlations.[10,24] The effective χ is given by the same form as eq 10 and is in general wave vector dependent. It implicitly differs from the corresponding homopolymer blend case since the block connectivity influences the interchain packing, and hence the direct correlation functions. Generalizations to treat other copolymer architectures (e.g., alternating, triblock, etc.) are straightforward. Random copolymers can also be potentially treated by introducing an extra approximation[21] to explicitly account for the quenched chemical disorder. Simple analytical results for the effective χ parameter at high temperature of isotopic 50/50 copolymers, as a function of microstructure, have been presented elsewhere.[21]

Following the work of Lowden and Chandler,[26] the polymer RISM integral equations can be formulated as a variational principle

$$\delta I_{RISM}/\delta C_{MM'}(r) = 0 \qquad r < d_{MM'} \quad (11)$$

where I_{RISM} is a functional of the direct correlation functions.[20] These direct correlation functions are parameterized as third-degree polynomials in the spatial variable r. Thus, for a binary blend, the variational principle in eq 11 leads to 12 coupled algebraic equations for the three sets of coefficients describing the three direct correlation functions. These algebraic equations are solvable by standard numerical methods.

III. Thermodynamics

Integral equation theories for liquids directly lead to structural information through the radial distribution functions $g_{MM'}(r)$ or structure factors $\hat{S}_{MM'}(k)$. From a knowledge of these pair correlation functions it is, in principle, possible to compute most thermodynamic functions of interest. The internal energy, representing the temperature dependence of the free energy, is easily obtainable as straightforward integrals over the pair potential function weighted by the appropriate radial distribution function.[27] For the case of simple monatomic liquids, the pressure, or volume dependence of the free energy, is related to an integral over $dg(r)/dr$. In the case of molecular liquids, on the other hand, the covalent bond constraint greatly complicates the calculation of the pressure from the radial distribution function and requires a knowledge of three-body correlation functions.[13,28-30] A more straightforward way of computing the pressure in blends is through the isothermal compressibility κ_T.

Following Kirkwood and Buff,[31] it is possible to express the compressibility of a molecular mixture in terms of the structure factors in eq 6 evaluated at zero wave vector

$$\kappa_T^{-1} = k_BT\sum_{\alpha\beta}\rho_\alpha\rho_\beta\hat{S}_{\alpha\beta}^{-1}(0) \quad (12)$$

where $\hat{S}_{\alpha\beta}^{-1}(0)$ are matrix elements of the inverse of the structure factor matrix in eq 7 evaluated at zero wave vector. This inverse matrix can be shown to be[19,20] given by

$$\hat{S}_{\alpha\beta}^{-1}(0) = (\delta_{\alpha\beta}/\rho_\alpha N_\alpha) - \hat{C}_{\alpha\beta}(0) \quad (13)$$

Substitution of eq 13 into eq 12 leads to a convenient expression for the compressibility of a polymer mixture.[32]

$$\kappa_T^{-1} = k_BT\sum_{\alpha\beta}[(\delta_{\alpha\beta}\rho_\alpha/N_\alpha) - \rho_\alpha\rho_\beta\hat{C}_{\alpha\beta}(0)] =$$

$$k_BT\left\{\frac{\rho_A}{N_A} + \frac{\rho_B}{N_B} - [\rho_A^2\hat{C}_{AA}(0) + \rho_B^2\hat{C}_{BB}(0) + 2\rho_A\rho_B\hat{C}_{AB}(0)]\right\} \quad (14)$$

The second line of eq 14 corresponds to the case of a binary

mixture of polymers. It should be emphasized that eq 14 is exact and depends only on the definition of the direct correlation functions through the generalized Ornstein–Zernike-like equations. Note that in the limit of zero density eq 14 correctly reduces to the ideal gas law. Equation 14 provides a convenient way to calculate the compressibility since the direct correlation functions are obtained naturally from solving the integral equations.

The isothermal compressibility of a mixture is defined at constant composition according to

$$\kappa_T \equiv -\frac{1}{V}\left(\frac{\partial V}{\partial P}\right)_{T,\phi} = \frac{1}{\eta}\left(\frac{\partial \eta}{\partial P}\right)_{T,\phi} \tag{15}$$

The pressure can then be determined by integrating the compressibility with respect to packing fraction under the constraint of constant volume fraction.

$$P = \int_0^\eta \frac{d\eta'}{\eta' \kappa_T}$$

In order to calculate thermodynamic properties or phase diagrams at constant pressure, the packing fraction $\eta(\phi)$ needs to be adjusted at each composition in order to hold the pressure constant. Such a procedure, although straightforward, is tedious and is beyond the scope of the present exploratory investigation on Gaussian chains.

It can be shown using standard thermodynamic identities that for a binary blend the specific Gibbs free energy $\tilde{F}$ is given by[33]

$$d\tilde{F} = -\tilde{S}\, dT + \tilde{V}\, dP + \left(\frac{\mu_A}{N_A \bar{v}_A} - \frac{\mu_B}{N_B \bar{v}_B}\right) d\phi \tag{16}$$

where the specific free energy $\tilde{F}$, entropy $\tilde{S}$, and volume $\tilde{V}$ are normalized by the molecular volume $V_0 = V\eta$ and the μ's are the chemical potentials of species A or B. The general spinodal condition for a binary blend can be written[33] in the form

$$\left(\frac{\partial^2 \tilde{F}}{\partial \phi^2}\right)_{T,P} = \frac{1}{N_A \bar{v}_A (1-\phi)}\left(\frac{\partial \mu_A}{\partial \phi}\right)_{T,P} = 0 \tag{17}$$

We now express the spinodal condition above in terms of the direct correlation functions. To this end we make use of the following results obtained by Kirkwood and Buff:[31]

$$\left(\frac{\partial \mu_\alpha}{\partial n_\beta}\right)_{T,P,n_{\gamma \neq n_\beta}} = N_\alpha N_\beta \hat{S}_{\alpha\beta}^{-1}(0) \tag{18a}$$

$$\left(\frac{\partial \mu_\alpha}{\partial n_\beta}\right)_{T,P,n_{\gamma \neq n_\beta}} = \left(\frac{\partial \mu_\alpha}{\partial n_\beta}\right)_{T,V,n_{\gamma \neq n_\beta}} - \frac{\bar{V}_\alpha \bar{V}_\beta}{V \kappa_T} \tag{18b}$$

$$\bar{V}_\alpha = N_\alpha \sum_\beta \rho_\beta \hat{S}_{\alpha\beta}^{-1}(0) \Big/ \sum_{\beta\gamma} \rho_\beta \rho_\gamma \hat{S}_{\beta\gamma}^{-1}(0) \tag{18c}$$

where n_M is the number of molecules of type M having N_M repeat units. Using eqs 12 and 18 together with the chain rule

$$\left(\frac{\partial \mu_A}{\partial \phi}\right)_{T,P} = \frac{V_0}{N_A \bar{v}_A}\left(\frac{\partial \mu_A}{\partial n_A}\right)_{T,P} - \frac{V_0}{N_B \bar{v}_B}\left(\frac{\partial \mu_B}{\partial n_B}\right)_{T,P}$$

gives the result

$$\frac{1}{N_A \eta k_B T}\left(\frac{\partial \mu_A}{\partial \phi}\right)_{T,P} = (\rho_B^2 \bar{v}_A^{-1} + \rho_A \rho_B \bar{v}_B^{-1}) \times (\hat{S}_{AA}^{-1}(0)\hat{S}_{BB}^{-1}(0) - \hat{S}_{AB}^{-1}(0)\hat{S}_{AB}^{-1}(0)) / (\rho_A^2 \hat{S}_{AA}^{-1}(0) + \rho_B^2 \hat{S}_{BB}^{-1}(0) + 2\rho_A \rho_B \hat{S}_{AB}^{-1}(0)) \tag{19}$$

By setting eq 19 equal to zero and making use of eq 13, we obtain the desired spinodal condition

$$\hat{\Lambda}(0) = 1 - \rho_A N_A \hat{C}_{AA}(0) - \rho_B N_B \hat{C}_{BB}(0) + \rho_A N_A \rho_B N_B [\hat{C}_{AA}(0)\hat{C}_{BB}(0) - \hat{C}_{AB}^2(0)] = 0 \tag{20}$$

This relation contains all the information required to describe UCST as well as LCST phase separation.

By comparison with eqs 7 and 8 we see that, at the spinodal condition, the three partial structure factors diverge at zero wave vector, a well-known result which is exploited in scattering experiments. We also see from eq 14 that, at the spinodal, the isothermal compressibility remains finite.[32] In the limit of an *incompressible* system, the isothermal compressibility is zero and it can be demonstrated that the spinodal condition in this case reduces to the zero wave vector limit of the RPA expression in eq 9.

$$\frac{1}{\hat{S}_{RPA}(0)} = \frac{1}{R^{1/2}\phi N_A} + \frac{R^{1/2}}{(1-\phi)N_B} - 2\hat{\chi}_s(0) = 0 \tag{21}$$

Besides the incompressible system, the RPA expression in eq 21 also rigorously applies to a 50/50 *symmetric isotope blend*. This follows from our previous analysis,[18,21,22] which shows that for a 50/50 symmetric isotope mixture the concentration fluctuations exactly decouple from the density fluctuations due to A ↔ B interchange symmetry. In this special case, the RPA spinodal condition in eq 21 applies even though the isothermal compressibility is nonzero. Limitations of the RPA analysis for compressible systems are also discussed by Freed and coworkers.[34]

IV. Symmetric Isotope Blend

We define a symmetric isotopic blend as one in which there is a complete symmetry in the structure of each of the components. In terms of our integral equation theory, this implies equal degrees of polymerization $N_A = N_B = N$, equal statistical segment lengths $\sigma_A = \sigma_B = \sigma$, and equal intramolecular structure $\hat{\omega}_A(k) = \hat{\omega}_B(k) \equiv \hat{\omega}(k)$ at all wave vectors. Furthermore, this model blend also requires a symmetry in the nonbonded interactions between like monomers (which we take to be zero for convenience) so that $v_{AA}(r) = v_{BB}(r) = 0$. Phase separation can be driven by an unfavorable $v_{AB}(r)$ interaction between unlike components, which we take to be of the form given by eq 4. Such an idealized "symmetric model" has been extensively studied recently by Sariban and Binder via Monte Carlo computer simulations of short chains on a lattice.[35] When $\epsilon_{AB}/k_B T < 0$, which is the usual case for dispersion interactions characteristic of nonpolar molecules, the phase-separated state is favored. The opposite case of $\epsilon_{AB}/k_B T > 0$ favors miscibility and could result from *specific* attractive interactions. Although it is not required, for simplicity we will use a *tangent sphere model* in which the statistical segment length and hard-sphere diameter are equal.

For a 50/50 symmetric blend, the A ↔ B interchange symmetry implies $C_{AA}(r) = C_{BB}(r)$ and $g_{AA}(r) = g_{BB}(r)$. This symmetry allows the three generalized Ornstein–Zernike-like equations, eq 1, to be reduced to two *decoupled* equations which describe intermolecular total density and concentration fluctuations, respectively.[19] The former is given by

$$\hat{h}_o(k) = \hat{C}_o(k)\hat{\omega}^2(k) + \rho\hat{\omega}(k)\hat{C}_o(k)\hat{h}_o(k) \tag{22}$$

where

$$\rho_A = \rho_B = \rho/2 \qquad \hat{C}_o(k) = (\hat{C}_{AA} + \hat{C}_{AB})/2$$
$$\hat{h}_o(k) = (\hat{h}_{AA} + \hat{h}_{AB})/2$$

Equation 22 with the associated closure conditions is of the form of an effective *homo*polymer melt. The pure intermolecular concentration fluctuations are described by

$$\rho\Delta\hat{h}(k) = \hat{\chi}_s(k)\hat{\omega}^2(k) + (\rho/2)\hat{\omega}(k)\hat{\chi}_s(k)\Delta\hat{h}(k) \quad (23)$$

where

$$\Delta\hat{h}(k) = (\hat{h}_{AA} - \hat{h}_{AB}) \qquad \hat{\chi}_s(k) = \rho(\hat{C}_{AA} - \hat{C}_{AB}) \quad (24)$$

with the unusual "core condition": $\Delta h(r) = 0$ for $r < \sigma$. Using the definition of the partial structure factors in eq 6, one can easily show that

$$\hat{S}_{AA}(k) = \rho[\hat{S}_o(k) + \hat{S}_{RPA}(k)] \quad (25)$$

where $\hat{S}_o(k)$ is the structure factor related to total density fluctuations in a reference homopolymer melt of density $\rho/2$

$$\hat{S}_o(k) = \hat{\omega}(k) + (\rho/2)\hat{h}_o(k)$$

Thus, for the case of a 50/50 symmetric isotope blend, the total density and concentration fluctuations decouple exactly. This provides a theoretical basis for the common experimental data analysis, i.e., background subtraction of homopolymer scattering followed by analysis with the incompressible RPA formula. Note, however, that this separation is only rigorous for the special 50/50 symmetric isotope case. Moreover, even in this situation, the incompressible RPA idealization that $\hat{S}_{AA}(k) = \hat{S}_{BB}(k) = -\hat{S}_{AB}(k)$ is not exact. In general, the full microscopic expressions given in eqs 7 and 8 should be employed.

Since the RPA formula is unambiguously applicable at 50% composition[19,21] for the symmetric isotope blend, it is meaningful to investigate trends in the effective χ parameter. The Flory–Huggins theory neglects the effect of chain connectivity and concentration fluctuations in the calculation of the nonideal free energy of mixing. We can think of this Flory–Huggins χ parameter, denoted by χ_o, as being a mean field approximation or *bare* χ *parameter* defined as[18,19]

$$\chi_o = \frac{3\eta}{\pi k_B T}[\hat{v}_{AA}(0) + \hat{v}_{BB}(0) - 2\hat{v}_{AB}(0)] = \frac{40\eta}{3T^*} \quad (26)$$

which is an off-lattice generalization of the usual definition, and the second equality follows from using the Lennard-Jones potentials given in eq 4. We define T^* in eq 26 as a reduced temperature $T^* = -k_BT/\epsilon_{AB}$. In contrast, our integral equation theory includes the effect of chain connectivity and concentration and density fluctuations in a nonperturbative fashion. The χ parameter defined in eq 10 will, in general, depend on variables such as composition and molecular weight through the direct correlation functions.

We solved the integral equations defined in eqs 1 and 3 numerically using standard methods discussed previously[8,20,26] for the case of the Gaussian, symmetric isotope mixture defined above. Figure 1 shows the relative composition dependence of the effective χ parameter calculated from eq 10 at various distances from the spinodal point. From the RPA formula in eq 9, the critical point occurs at $\phi = 0.50$ when $N\chi_{0.5} = 2$, where $\chi_{0.5}$ is the effective χ parameter at 50% composition. Each of the curves in Figure 1 is for a constant reduced temperature where T^* is chosen to give a particular value for the product

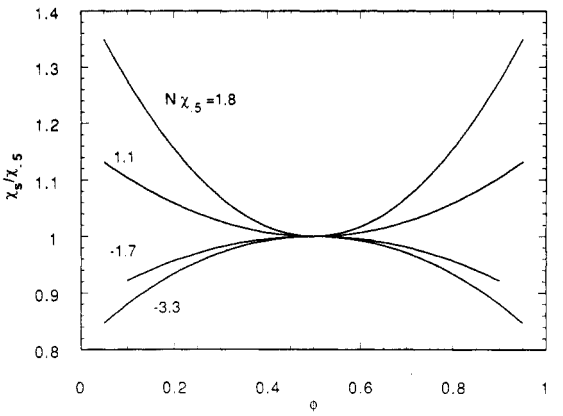

Figure 1. Composition dependence of the χ parameter for the symmetric isotopic blend, relative to the 50% mixture, at various fixed temperatures for chains of 500 units. Each temperature was chosen to give the $N\chi_{0.5}$ values indicated. The packing fraction was held fixed at $\eta = 0.45$. Curves for which $N\chi_{0.5} > 0$ correspond to a partially miscible blend, whereas completely miscible mixtures occur when $N\chi_{0.5} < 0$.

$N\chi_{0.5}$. It can be seen that the composition dependence is symmetric about the 50/50 mixture and the curves become steeper as the spinodal is approached. It should be noted that for our definition of χ through the direct correlation functions, χ_s remains bounded in the $\phi = 0, 1$ limits. It can be seen for positive $N\chi_{0.5}$ ($T^* > 0$) the interactions are destabilizing and the composition profiles are parabolic, concave up with the equal composition blend being the most stable. The reverse occurs when $N\chi_{0.5}$ is negative resulting from favorable interactions. In this case, the system exhibits complete miscibility for any $T^* = -k_BT/\epsilon_{AB} < 0$, although concentration fluctuations now *decrease* the relative magnitude of the stabilizing interactions.

One of the consequences of chain connectivity and concentration fluctuations for the $T^* > 0$ case is that the miscibility of the system is increased. By allowing local fluctuations in concentration, the system can lower its free energy without undergoing macroscopic (at $k = 0$) phase separation. As a result, the effective χ parameter is *renormalized* downward relative to the *bare*, Flory–Huggins χ of eq 26. Thus we expect that the UCST temperature will be lower than in the Flory–Huggins theory. From an approximate analytical treatment in the high-temperature limit (*Gaussian string model*) given previously,[21,22] we have shown that the renormalization ratio, χ_s/χ_o, is molecular weight dependent and has the following form[21] for the symmetric isotope blend:

$$\chi_s/\chi_o \sim 1.63N^{-1/2} \quad (27)$$

which is valid for long chains. The same qualitative form applies at low temperatures (i.e., $T \to T_c^+$). This unexpected molecular weight dependence of the renormalization ratio in eq 27 is counterintuitive to the classical notion that χ is a local quantity of energetic origin. The reduction of χ by $\sqrt{N}$, a factor proportional to the radius of gyration, is a clear prediction from our RISM-MSA theory and appears to be independent of factors such as the particular choice of the potential function or the local details of the intramolecular structure.[21,22] The origin of this rather startling effect is due to the stabilizing influence of weak, but long-range (on a scale of R_G), fluctuations in intermolecular concentration. Because of the *correlation hole* effect[23] in polymers, local fluctuations in intermolecular packing are predicted to be propagated out to length scales comparable to the radius of gyration. For this reason, χ cannot be viewed as solely a local energetic quantity but depends on R_G. Moreover, the relevance of such long-range fluctuations is very sensitive[22] to both spatial

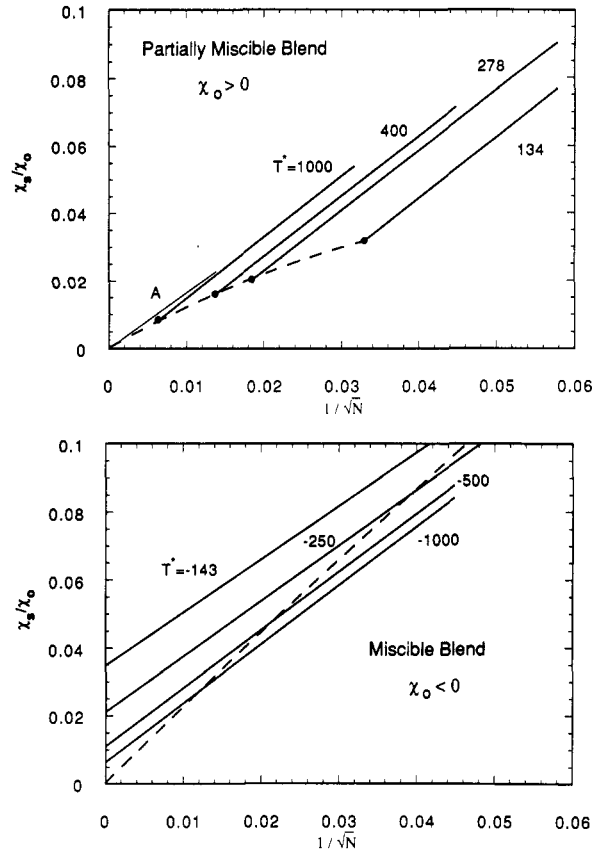

Figure 2. Generalized χ parameter χ_s relative to the Flory–Huggins χ_o versus $N^{-1/2}$ for various symmetric isotopic mixtures at 50% composition with $\eta = 0.45$. The solid lines refer to calculations at fixed reduced temperatures T^*. (a) Partially miscible blend: For the dashed curve, the temperature is adjusted so that $N\chi_{0.5} = 2.00$. Curve A is the analytical prediction from eq 27. (b) Miscible blend: The dashed curve corresponds to $N\chi_{0.5} = -2.00$.

dimension and fractal topology of the polymer chains analogous to the problem of critical phase transitions. An important consequence of this predicted nonlocal behavior of χ is that for ideal coils in three dimensions the spinodal temperature T_c^* scales with $\sqrt{N}$, in contrast to the linear dependence on N predicted from the Flory–Huggins theory. From eqs 26 and 27, an analytical approximation to the critical temperature for a symmetric isotopic mixture of Gaussian strings at $\phi = 0.50$ is given by[21]

$$T_c^* \sim 10.87\eta\sqrt{N} \tag{28}$$

Figure 2a shows the numerical results for a partially miscible blend of Gaussian chains at various fixed, reduced temperatures $T^* > 0$. Obviously the critical point will eventually be reached as the degree of polymerization is increased at fixed temperature. This stability limit is shown by the dashed curve in Figure 2a, which represents the spinodal line. Phase separation will occur at each of the fixed temperatures at the intersection with the dashed curve, indicated by the filled circles. The dashed curve can be viewed as the renormalization ratio determined numerically by adjusting the temperature T^* at each N in order to hold $N\chi_s = 2$. Note that at high temperatures, numerical results compare favorably with curve A, the analytical approximation of eq 27.

It can be seen from Figure 2a that the generalized χ parameter is inversely proportional to $\sqrt{N}$ over the range of molecular weights studied. It is interesting to note, however, that each of the isotherms extrapolates to an apparent negative intercept as $N \to \infty$. From our previous analytical calculations on the *Gaussian thread model*,[21]

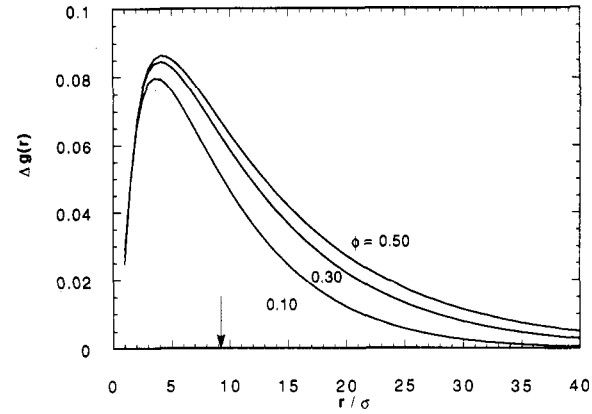

Figure 3. Measure of the nonrandomness of the intermolecular packing, $\Delta g(r) \equiv 0.5[g_{AA}(r) + g_{BB}(r) - 2g_{AB}(r)]$, for symmetric isotope mixtures at the three compositions indicated for $N = 500$, $T^* = 134$, and $\eta = 0.45$. The radius of gyration is indicated by the arrow. The contact values, $\Delta g(\sigma)$, are 0.02479, 0.02703, and 0.02905 for $\phi = 0.1$, 0.3, and 0.5, respectively.

we have shown that this infinite chain intercept should be proportional to $1/T^*$. Of course the spinodal curve intervenes at finite N. Only in the infinite temperature limit would the isothermal lines extrapolate to a renormalization ratio of zero.

Figure 2b is a similar plot of the renormalization ratio for a fully miscible symmetric isotopic blend determined numerically for a series of constant temperatures $T^* < 0$. In this case both χ_o and χ_s are negative, indicating complete absence of a UCST. It should be mentioned that since the numerical calculations were performed at constant density (or packing fraction η) rather than at constant pressure, we cannot rule out possible LCST behavior.[33] In Figure 2b the dashed curve represents the renormalization ratio at $N\chi_s = -2$. Note that the dashed curve determined at a constant $N\chi_s$ extrapolates to a zero intercept in contrast to the lines at fixed, finite temperature. It can also be seen in Figure 2b that, for the miscible blend also, the generalized χ parameter at fixed temperature is inversely proportional to $\sqrt{N}$. In this case, however, fluctuations *increase* the effective χ_s (although it remains negative) thereby destabilizing the blend relative to the mean-field behavior.

As stated above, the origin of the predicted nonclassical behavior, such as the composition and molecular weight dependence of χ in mixtures, is due to relatively long range ($\sim R_G$) fluctuations in intermolecular concentration caused by the correlation hole. One measure of this "nonrandomness" of the packing is given by $\Delta g(r) \equiv 0.5[g_{AA}(r) + g_{BB}(r) - 2g_{AB}(r)]$. $\Delta g(r)$ is a measure of the average tendency of similar intermolecular pairs of monomers to be at a distance r apart relative to dissimilar pairs. Of course, for the random mixing situation as assumed in the Flory–Huggins theory, $\Delta g(r)$ is identically zero on all length scales. $\Delta g(r)$ is plotted in Figure 3 for a symmetric isotopic mixture of Gaussian chains of $N = 500$ units for three compositions. It can be seen that the correlations are relatively weak ($\Delta g_{max}(r) < 0.1$) but they persist over distances in excess of R_G. Analytic calculations suggest[21] that $\Delta g_{max} \propto (\chi_s N)N^{-1/2}$ in the long-chain limit. We can also observe from Figure 3 that the concentration fluctuations are maximum for the 50/50 mixture. Figure 4 is a similar plot of $\Delta g(r)$ for five different mixtures defined in the figure caption. It can be noticed for the partially miscible mixtures B, C, and E that $\Delta g(r) > 0$, indicating a tendency for chains of like species to be in proximity, even though macroscopic phase separation has not yet occurred. In contrast, the miscible mixtures A and D exhibit the opposite tendency as expected since interac-

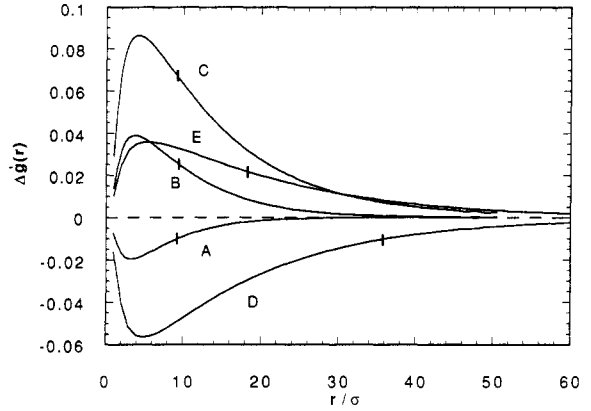

Figure 4. Measure of the nonrandomness of the intermolecular packing, $\Delta g(r) \equiv 0.5[g_{AA}(r) + g_{BB}(r) - 2g_{AB}(r)]$, for various symmetric isotope mixtures at $\eta = 0.45$ and $\phi = 0.5$. The curves are as follows: (A) $N = 500$, $T^* = -500$; (B) $N = 500$, $T^* = 278$; (C) $N = 500$, $T^* = 134$; (D) $N = 8000$, $T^* = -250$; (E) $N = 2000$, $T^* = 400$. The radii of gyration are marked on each curve by a vertical dash.

tions between unlike species are favorable. It can also be observed in Figure 4 that the range of the correlations increases significantly with N, but the location of the extremum in $\Delta g(r)$ is more weakly dependent on molecular weight. This is consistent with our approximate analytical theory,[21] which predicts that the maximum in $\Delta g(r)$ occurs at $r = R_{max} \propto N^{1/4}$ for $\phi = 0.50$. Hence the length scale corresponding to the largest fluctuations occurs well inside the radius of gyration for long polymer chains.

The effective χ parameters shown in Figures 1 and 2 were calculated from eq 10 by taking the thermodynamic limit of $k \to 0$. In scattering experiments, however, it is conceivable that the wave vector dependence of the direct correlation functions could affect the χ parameter, and hence the structure factor, in an experimentally observable range. To address this question, we calculated the wave vector dependent $\hat{\chi}_s(k)$ from eq 10 for the same five mixtures in Figure 4. The relative wave vector dependence of χ out to large angles is displayed in Figure 5a. It can be seen from the insets in Figure 5a and Figure 5b that the χ parameter can exhibit a significant dependence on k even in the region $kR_G \cong 1$. There is a very large wave vector dependence at large angles, including a sign change. The latter features are in qualitative accord with previous findings for dense homopolymer melts of flexible chains and rings.[8,10,11] In general, the amount of wave vector dependence in χ at small angles is larger for the partially miscible blends ($T^* > 0$) relative to the fully miscible ($T^* < 0$) mixtures.

As seen in Figure 5b, there are also interesting dependences of the magnitude of the $kR_G \cong 1$ "curvature effects" [19] on degree of polymerization and proximity to the phase separation point (see inset). At fixed N, as the spinodal is approached (increasing $\chi_s N$), the k dependence of $\hat{\chi}_s(k)/\chi_s$ increases. At fixed $\chi_s N$, however, analysis of the data in Figure 5b reveals that the magnitude of the initial slope decreases linearly with $N^{-1/2}$ and extrapolates to zero. From a curve fit to the data in Figure 5b (at $\chi_s N = 1.8$) we find

$$\frac{\hat{\chi}_s(k)}{\chi_s} \cong 1 - 0.14\sqrt{\frac{200}{N}}(kR_G)^2 + \ldots \qquad (29a)$$

or using the large N relation $\chi_s \propto \chi_o N^{-1/2}$, one obtains a result of the form

$$\hat{\chi}_s(k) = \chi_s - (\text{constant})\chi_o(k\sigma)^2 + \ldots \qquad (29b)$$

implying the initial curvature is N independent for long Gaussian chains.

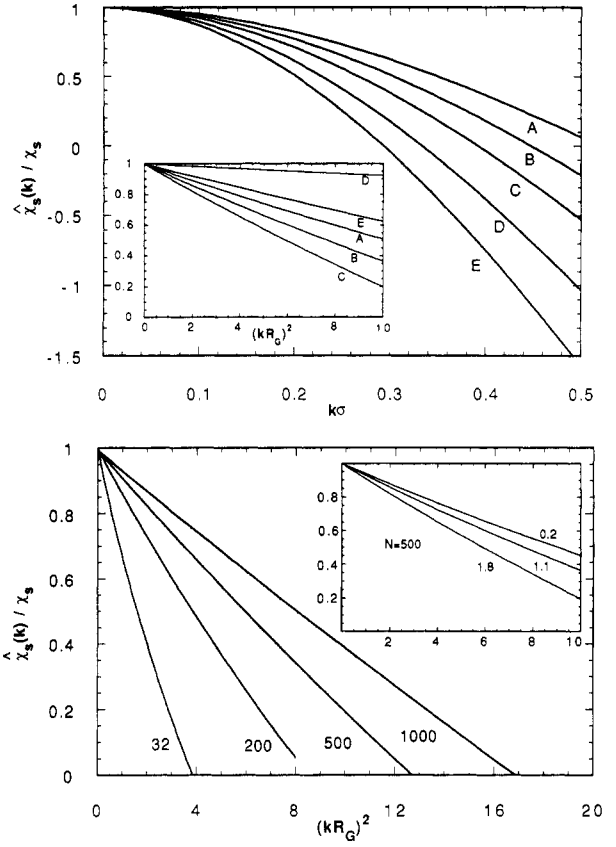

Figure 5. Generalized χ parameter $\hat{\chi}_s(k)$, relative to its zero wave vector value $\chi_s \equiv \hat{\chi}_s(0)$, as a function of dimensionless wave vector. (a, top) Results are plotted versus $k\sigma$ for the same cases (A–E) described in Figure 4. The inset shows the results plotted versus $(kR_G)^2$. (b, bottom) Results are plotted versus $(kR_G)^2$ for various degrees of polymerization at a fixed distance from the spinodal ($N\chi_{0.5} = 1.8$). The inset displays the behavior at various distances from the spinodal $N\chi_{0.5}$ at fixed $N = 500$.

In practice, many SANS experiments probe relatively small valus of $k\sigma$ and it appears that χ does not significantly vary in this range. This can be seen explicitly by including the curvature term in the RPA expression for the 50% symmetric isotope blend. For the case of $\chi_s N = 1.8$ one obtains

$$\hat{S}_{RPA}^{-1}(k) = 4\hat{\omega}^{-1}(k) - 2\chi_s - (k\sigma)^2\hat{\chi}_s''(0) = 2\left[\frac{2}{N} - \chi_s\right] + \frac{(k\sigma)^2}{3}\left[1 + (0.14)\chi_s N\sqrt{\frac{200}{N}}\right] \qquad (30)$$

where the second line follows from employing a Gaussian form (valid for $k\sigma \ll 1$) for $\hat{\omega}(k)$ and eq 29a has been used. From eq 30 one sees that curvature effects in $\hat{\chi}_s(k)$ can be viewed as "renormalizing" the apparent statistical segment length.[19] However, this correction is generally small; e.g., for an $N = 2000$ chain there is a ~4% correction to σ. For most systems such a correction would not be outside experimental error. Moreover, local, single-chain corrections to the Flory ideality ansatz are likely to be of this size or larger. It should be pointed out, however, that Brereton and co-workers[36] have reported a very large wave vector dependent χ in some polymer mixtures based on SANS measurements. Although the k dependence of the χ parameter is not a significant factor in describing the thermodynamics of macroscopic blend systems, it may be relevant in certain phase-separation processes where microscopic features are present, such as in the early stages of spinodal decomposition, microphase separation in block copolymers, and phase separation near surfaces. A wave vector dependence of χ for moderately sized diblock

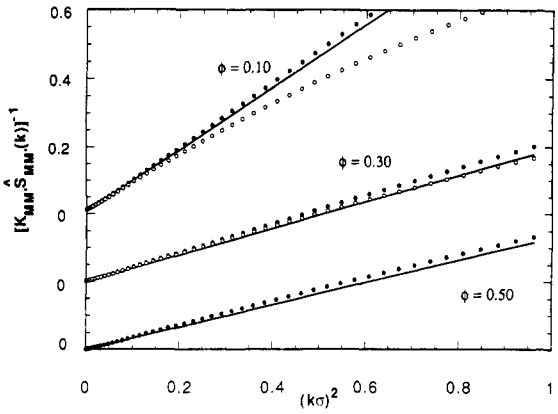

Figure 6. Reciprocal structure factor versus the square of the wave vector for symmetric isotope mixtures at the three compositions indicated for $N = 500$, $T^* = 134$, and $\eta = 0.45$. The filled and open circles refer to $\hat{S}_{BB}(k)$ and $\hat{S}_{AA}(k)$, respectively. For the $\phi = 0.50$ mixture, $\hat{S}_{BB}(k) = \hat{S}_{AA}(k)$. The normalization coefficient defined in the text is $K_{AA} = K_{BB} = v_A/\eta$ for the symmetric isotopic blend. The solid lines refer to the RPA approximation calculated with the zero wave vector χ parameter. Note that the vertical axes are displaced for clarity. The intercepts at zero wave vector are as follows for $\phi = 0.1$, (0.3), [0.5]: 0.0126, 0.012 15, 0.013 06, (0.001 74, 0.001 71, 0.001 85), [0.000 816, 0.000 816, 0.000 816] for the $\hat{S}^{-1}_{AA}(k)$, $\hat{S}^{-1}_{BB}(k)$, and $\hat{S}^{-1}_{RPA}(k)$ results, respectively.

copolymers can lead to significant molecular weight and temperature dependence of the location of the $k^* \neq 0$ maximum of $\hat{S}(k)$ in the disordered phase, as recently observed experimentally[41] and in Monte Carlo simulations.[42] Such a wave vector dependence will also modify the microphase transition behavior.

It should be emphasized again that the widely used RPA formula of de Gennes in eq 9 is strictly valid in only two cases: (1) a hypothetical incompressible system ($\kappa_T = 0$) and (2) a symmetric isotopic blend at 50% composition for which the effective homopolymer melt background scattering has been subtracted. This limitation is illustrated in Figure 6, where we have plotted the reciprocal structure factor of Gaussian chains for three different compositions. The points represent the results calculated from the exact expressions in eqs 7 and 8 whereas the lines are from the RPA expression using the zero wave vector χ parameter in eq 10. It can be seen from the figure that at $\phi = 0.50$ there is a single structure factor $\hat{S}_{AA}(k) = \hat{S}_{BB}(k)$. If the wave vector dependence of the χ parameter is included in the RPA calculation, then we find to very high accuracy that $\hat{S}_{RPA}(k) = \hat{S}_{AA}(k) = \hat{S}_{BB}(k)$. Note that off 50% composition that differences between $\hat{S}_{AA}(k)$ and $\hat{S}_{BB}(k)$ are evident, particularly at higher wave vectors. This signals a breakdown in the RPA expression since there is no longer a single, unique structure factor. Nevertheless, for the symmetric isotope blend of Gaussian chains studied, the deviations are small in the experimentally relevant region of wave vector.

V. Structural Asymmetry

We chose the term *symmetric isotopic* blend to describe a mixture of structurally symmetric chains because an approximate experimental realization is provided by a mixture of deuterated/hydrogenated polymers. Mixtures of this type have been studied extensively by Bates and co-workers.[37,38] For such a mixture, the structures of the deuterated (D) and hydrogenated (H) polymers are close to being symmetric,[37] with statistical segment lengths $\sigma_H \cong 1.001\sigma_D$ and interactions $v_{HH}(r) \cong 1.04v_{DD}(r)$. For our present purposes we will neglect these small asymmetries. SANS measurements on isotopic mixtures of poly(ethylethylene) (PEE) and poly(vinylethylene) (PVE) by Bates and co-workers,[38] when analyzed via the RPA formula, yield a composition dependence for χ in qualitative agreement with our predictions in Figure 1 for the symmetric isotope blend. Careful examination of these experimental results for χ, however, does reveal puzzling asymmetries in the composition dependence.

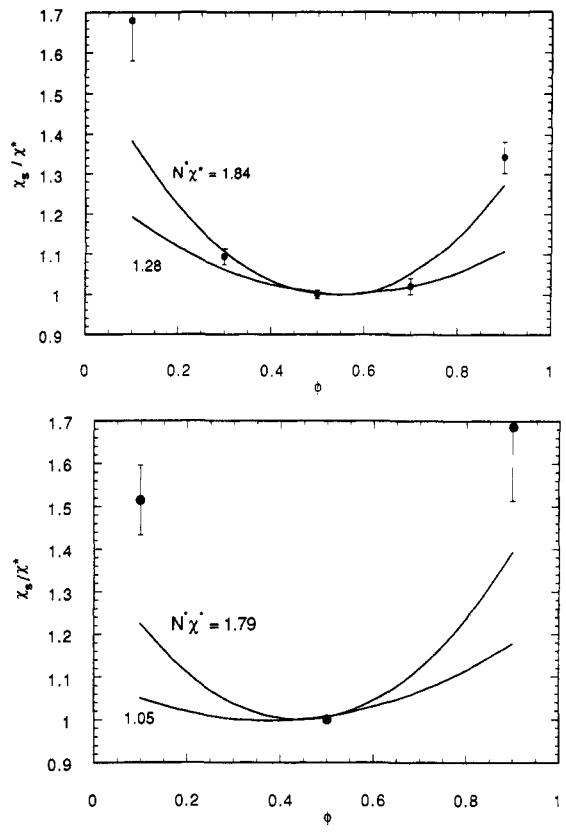

Figure 7. Comparison between calculated and measured χ parameters relative to the $\chi^* = \chi_S(\phi^*)$ at the critical composition ϕ^*. ϕ is the volume fraction of the deuterated chains, and the packing fraction was held fixed at $\eta = 0.45$. Points and error bars are from SANS data in ref 3 for PEE isotopic mixtures. Lower curves are theoretical results with T^* chosen so that $N^*\chi^*$ is close to the experimental values. Upper curves are for T^* chosen closer to the spinodal: (a, top) $N_D = 2620$, $N_H = 3280$; (b, bottom) $N_D = 2620$, $N_H = 1596$.

A possible source of this observed skewness in the composition dependence of χ is due to differences in molecular weight. In their study,[38] Bates and co-workers intentionally varied the molecular weight of the components, thus breaking the symmetry in the structure at a global scale. We have attempted to model the PEE system by performing numerical calculations for Gaussian chain mixtures with the ratios of molecular weights $R_N \equiv N_H/N_D$ corresponding to the experimental blends. Parts a and b of Figure 7 show the relative composition dependence of χ for $R_N = 1.25$ and $R_N = 0.61$, respectively. Since the molecular weights are not equal, the composition ϕ^* at the critical point no longer occurs at $^1/_2$. An estimate of ϕ^* can be made by using the RPA formula in eq 9 and neglecting the composition dependence of χ near ϕ^*.

$$\phi^* = (R_N - \sqrt{R_N})/(R_N - 1) \tag{31a}$$

We also define an effective number of skeletal bonds N^* in order to ensure that $N^*\chi^* = 2$ at the critical point

$$N^* = 4N_D R_N \phi^*(1-\phi^*)/[\phi^* + R_N(1-\phi^*)] \tag{31b}$$

where $\chi^* = \chi_s(\phi^*)$. In Figure 7 the points and error bars correspond to the SANS determined χ (normalized by χ^*) of Bates and co-workers.[38] The solid curves correspond to our calculations at two reduced temperatures T^* chosen

to give the $N^*\chi^*$ values indicated in the figures. The lower $N^*\chi^*$ values in Figure 7 correspond to the experimentally measured values. It can be seen from Figure 7a that when $N_H > N_D$ the curves become skewed so that $\chi_s(\phi) > \chi_s(1-\phi)$ in qualitative agreement with the experimental data. Likewise, when $N_H < N_D$ in Figure 7b, the reverse is true for both the theoretical prediction and the data. In both cases, however, it can be seen that the theory underestimates the magnitude of the composition dependence, even at lower temperatures (upper curves) closer to the spinodal. This lack of quantitative agreement between our theory and experiment may be attributable to the Gaussian approximation for the intramolecular structure and/or to our assumption that $v_{HH}(r) = v_{DD}(r)$. Of course, it should be kept in mind that the concentration dependence of χ_s is a relatively small effect and accurate experimental determination via SANS is difficult, particularly away from 50% composition, where diminished signal intensity introduces larger uncertainties. Moreover, the accuracy of a literal RPA description in the data analysis, and hence the precise molecular meaning of a single χ parameter, deteriorates systematically as the compositional asymmetry increases and density fluctuations become relatively more important. In this case additional cross terms appear in eq 25 which couple together density and concentration fluctuations. These subtle effects will be investigated in future studies which include $\hat{\omega}_A(k)$ and $\hat{\omega}_B(k)$ functions which more realistically reflect the intramolecular structure of the PEE chains. It should be mentioned that similar qualitative agreement was also found for the PVE mixtures in ref 38, although the comparison is not shown here.

It should be pointed out that Bates and co-workers[38] did report differences in the SANS-determined χ parameters for both the PEE and PVE mixtures consisting of different molecular weight combinations of the hydrogenated and deuterated species. For PEE consisting of degrees of polymerization n_D = 1310 monomers mixed with n_H = 798 (PEE13) and n_H = 1640 (PEE12), the ratio of χ parameters for the 50/50 mixture (χ_{13}/χ_{12}) was 1.10 ± 0.04. In the case of 50/50 PVE mixtures with n_D = 1270, n_H = 791 (PVE13), and n_H = 1690 (PVE12), the corresponding χ ratio was measured as 1.14 ± 0.07. Numerical calculations on Gaussian chain blends yield corresponding ratios of 1.24 and 1.23, whereas previous analytical computations[21] predicted 1.16 and 1.19 for PEE and PVE mixtures, respectively. Our previous analytical calculations also indicate that the χ parameter ratios decrease slightly as the range of the potential increases. The numerical calculations were performed with the Lennard-Jones 6–12 potential in eq 4. Such comparisons of our theoretical predictions of the molecular weight dependence of the χ parameter with the SANS determined χ's of Bates and co-workers[38] are suggestive of nonclassical behavior in eqs 27 and 28. Clearly, a systematic study of isotopic mixtures over a wide molecular weight range is needed in order to make definitive statements regarding the validity of our predictions for the molecular weight dependence of blend miscibility.

We now consider the consequences when we break the symmetry in the local structure by allowing $\gamma = \sigma_B/\sigma_A \neq 1$. We expect the RPA approximation in eq 9 to become systematically poorer as γ deviates from unity. Keeping this in mind, we examine the trends in the χ parameter defined in eq 10 as the monomer size becomes asymmetric between the two components. Such a mixture represents the vast majority of polymer blends that one encounters in the laboratory. In Figure 8a we have depicted how the χ parameter changes ($N_A = N_B = 500$), at fixed temperature, when γ is systematically increased. Starting with

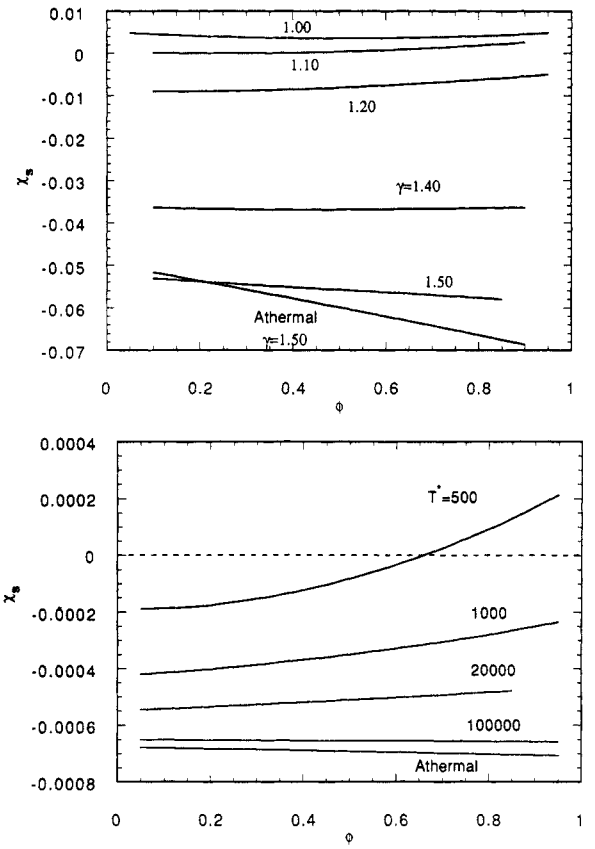

Figure 8. χ parameters calculated from eq 10 as a function of the volume fraction ϕ of the A component for structurally asymmetric polymer mixtures: (a, top) $N_A = N_B = 500$, $T^* = 134$ for various asymmetry ratio γ; (b, bottom) $N_A = N_B = 2000$, $\gamma = 1.05$ for various reduced temperatures T^* and $\eta = 0.45$.

the symmetric isotope blend ($\gamma = 1$), which is a shallow, symmetric parabola on this scale, the composition dependence becomes skewed with χ decreasing rapidly as γ increases from unity. Note that for γ in excess of about 1.1, χ becomes negative. Also shown for comparison is χ for the athermal mixture,[20] which represents the infinite temperature limit where attractive interactions become insignificant. In this athermal regime the dominance of local noncombinatorial entropic (packing) factors results in a spatially much shorter range $\Delta g(r)$ correlation pattern,[20] which is qualitatively distinct from the isotopic blend behavior shown in Figures 3 and 4.

A similar plot is shown in Figure 8b for the $N_A = N_B = 2000$ system at fixed $\gamma = 1.05$. This figure shows how the composition-dependent χ parameter changes as the temperature is systematically lowered from the infinite-temperature, athermal limit. It can be observed that as T^* decreases χ increases and the slope of the curves changes from negative to positive. Note that, at $T^* = 500$, χ changes from negative to positive over the composition range, indicating an apparent miscibility gap.

One model asymmetric isotopic system, the deuterated polystyrene/poly(*p*-methylstyrene) blend, has been studied[39] by Jung and Fischer using SANS. These authors analyzed their scattering data using the RPA approach and observed a χ parameter for a 50/50 mixture of the form

$$\chi_s = -(0.0002 \pm 0.0001) + (2.16 \pm 0.06)/T \quad (32)$$

In order to compare our studies with these experiments, we calculated the χ parameter as a function of reduced temperature, with appropriate parameters to match the Jung–Fischer system. In Figure 9 we show χ as a function of $1/T^*$ over a wide range of temperatures including the

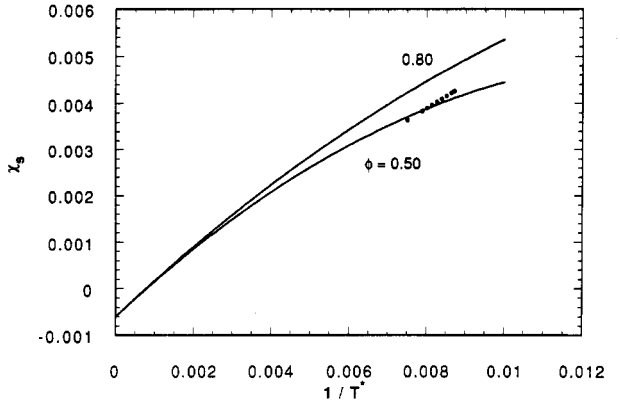

Figure 9. χ parameters calculated from eq 10 as a function of $1/T^*$ for the conditions $N_A = 290$, $N_B = 470$, $\gamma = 1.03$, and $\eta = 0.45$. The curves represent the theoretical results at the two compositions indicated. The points are SANS data from Jung and Fischer[38] on the deuterated polystyrene/poly(*p*-methylstyrene) blend system represented by eq 26. The degrees of polymerization are approximately the same as the calculation and $\phi = 0.5$. The experimental temperature was scaled relative to T^* by adjusting the experimental and theoretical χ's to be the same at a particular temperature as seen in the figure.

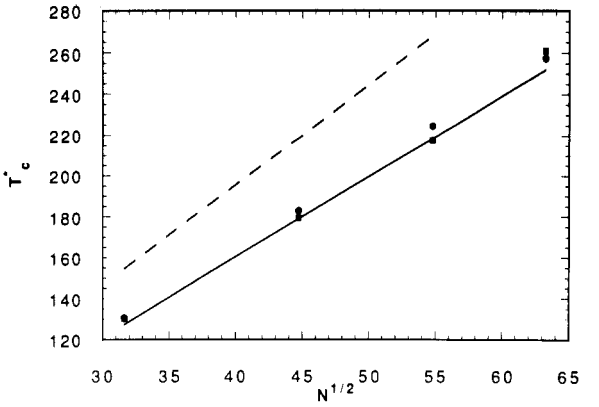

Figure 10. Critical temperature T^*_c versus $\sqrt{N}$ for three different asymmetry ratios γ, $\phi = 0.5$, and $\eta = 0.45$. The squares correspond to the symmetric blend $\gamma = 1.0$ and the circles are for $\gamma = 1.05$. The solid line is a least-squares fit to the $\gamma = 1.10$ calculations. The dashed line is the analytical approximation in eq 28.

athermal limit. In this figure the experimental SANS data are also plotted, where the temperature in eq 32 was scaled to the reduced temperature T^* in order to match the theoretical prediction at one arbitrary temperature. It can be seen that the theory predicts a pronounced curvature in the $1/T^*$ dependence of χ when viewed over a wide temperature range. For an experimentally accessible range of temperatures, such as shown for the Jung–Fischer data, an approximate $1/T^*$ dependence is found. It should be mentioned that because our theory uses the MSA closure in eq 3, the critical exponent for temperature-induced divergences characteristic of the nonclassical spherical model applies, which is known to be too large. Nevertheless, we do expect, on general physical grounds, some curvature of the type found in Figure 9 to exist due to stabilizing fluctuation effects. Depending on the particular experimental system and conditions, this curvature effect can lead to an *apparent* infinite temperature intercept which could be positive or negative, depending on the range of temperature over which the linear extrapolation is made. This suggests that in representing χ in the form $A + B/T$, it is not always correct to think of A as being the *athermal* entropic contribution as is often done in the literature.

Examination of Figure 8 seems to suggest that if the RPA is valid, a strategy for increasing the miscibility of a blend would be to increase the disparity in monomer size between components. Such a notion is contrary to the commonly held belief that "like dissolves like". In order to investigate this interpretation further, we attempted to numerically calculate the critical temperature T_c^* as a function of molecular weight using the exact spinodal condition in eq 20, which includes nonzero *compressibility* effects. We encountered serious numerical difficulties near the critical point because our algorithm for solving the polymer RISM equations fails when $\hat{\Lambda}(k)$, defined in eq 8, is less than or equal to zero for any wave vector k. From eq 20 we see that it is unfortunately in this region near $\hat{\Lambda}(0) = 0$ where we need to find solutions. In order to extrapolate to the critical point we made use of the analytical result[21,22] for the symmetric isotope blend which states

$$\hat{S}_{RPA}^{-1/2}(0) \propto \xi_\phi^{-1} \propto T^* - T_c^*$$

where ξ_ϕ is the concentration fluctuation correlation length. We assume that the same spherical model scaling also applies to the weakly unsymmetrical blend and determine T_c^* by extrapolating $[\hat{S}_{AA}(0)]^{-1/2}$ versus T^* to zero.

Table I
N_c at Fixed $T^* = 134$

γ	N_c	$N_c\chi_s$
1.00	1026	2.00
1.02	1025	1.87
1.05	1036	1.21
1.07	1025	0.49

The results for T_c^* determined by extrapolation are shown in Figure 10 as a function of $\sqrt{N}$ for the symmetric isotope blend and two unsymmetric cases $\gamma = 1.05$ and 1.10. The solid line is a least-squares fit to the $\gamma = 1.10$ mixture. Note that increasing γ from unity only slightly decreases the spinodal temperature. A qualitatively similar (but larger) effect was calculated by Malescio[40] on atomic mixtures of Lennard-Jones particles of unequal size based on a solution of the hypernetted chain integral equations. Thus we see from Figure 10 that we do not obtain the massive stabilization predicted on the basis of the RPA approximation and the χ parameters in Figure 8. In fact, the χ parameters corresponding to the unsymmetric mixtures in Figure 10 are actually negative, implying complete miscibility. It is important to point out that T_c^* is proportional to the *square root* of N rather than the linear N dependence expected from the Flory–Huggins theory. The dashed line in Figure 10 is the analytical prediction from eq 28 based on the Gaussian string model.[21] The analytical result is remarkably close to the numerical calculations, considering the simplifying approximations made.

In another series of calculations we attempted to determine the critical degree of polymerization N_c for phase separation of a system at fixed temperature $T^* = 134$ for various asymmetries γ. The results are shown in Table I. It can be seen that N_c is fairly insensitive to γ; however, because of uncertainties in the extrapolation it is difficult to establish a clear trend and more work is necessary to quantitatively clarify the situation. Nevertheless, we can generally conclude from the third column of the table that the RPA prediction of $N_c\chi_s = 2.0$ at the spinodal becomes inadequate as γ increases from unity.

VI. Discussion

It is clear from the results in Figure 10 and the table that the RPA calculation, with the χ parameter defined as in eq 10, gives very poor predictions for the phase behavior of Gaussian chains of unequal statistical segment

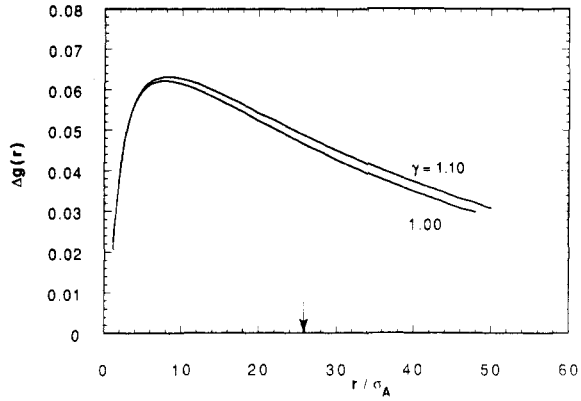

Figure 11. Measure of the nonrandomness of the intermolecular packing, $\Delta g(r) \equiv 0.5[g_{AA}(r) + g_{BB}(r) - 2g_{AB}(r)]$, for a blend of $N_A = N_B = 4000$, $T^* = 273$, $\phi = 0.5$, and $\eta = 0.45$. The curves correspond to the symmetric blend $\gamma = 1.0$ and the asymmetric mixture $\gamma = 1.10$, as shown in the figure. The radius of gyration of the A component is indicated by the arrow. The contact values, $\Delta g(\sigma)$, are 0.022 56 and 0.020 60 for $\gamma = 1.10$ and 1.00, respectively.

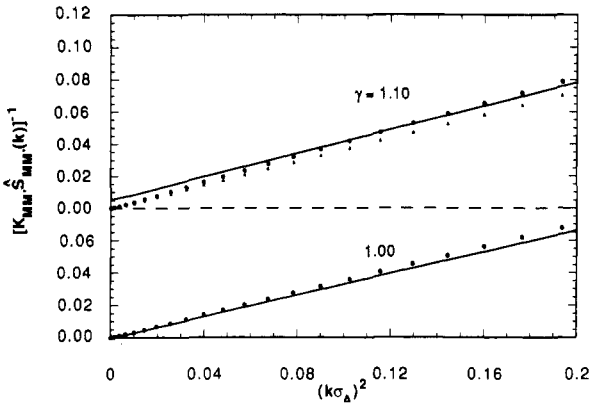

Figure 12. Reciprocal structure factor versus the square of the wave vector for blends of $N_A = N_B = 4000$, $T^* = 273$, $\phi = 0.50$, and $\eta = 0.45$ at the two values of γ indicated. The normalization coefficients defined in the text are $K_{AA} = v_A/\eta$ and $K_{BB} = v_B/\eta$. The circles and triangles refer to $\hat{S}_{AA}(k)$ and $\hat{S}_{BB}(k)$, respectively. For the $\gamma = 1.0$ mixture, $\hat{S}_{BB}(k) = \hat{S}_{AA}(k)$. The solid lines refer to the RPA approximation calculated with the zero wave vector χ parameter. Note that the vertical axis is displaced for clarity. The zero wave vector structure factors are as follows: $\hat{S}_{AA}(0) = \hat{S}_{BB}(0) = \hat{S}_{RPA}(0) = 3.975 \times 10^5$ for the $\gamma = 1.0$ mixture; $\hat{S}_{AA}(0) = 2.0191 \times 10^5$, $\hat{S}_{BB}(0) = 2.2539 \times 10^5$, $\hat{S}_{RPA}(0) = 186.61$ for the γ 1.10 case.

size ($\gamma \neq 1$). In order to investigate this behavior further we calculated $\Delta g(r)$, the nonrandomness of the packing, for both symmetric and asymmetric isotopic chain mixtures ($\phi = 0.5$) of 4000 units near the critical point T_c^*. This comparison is depicted in Figure 11. Despite the huge difference in χ_s between the two mixtures (χ_s = 0.000 465 and −0.00217 for $\gamma = 1.00$ and 1.10, respectively) their intermolecular structure, as evidenced by $\Delta g(r)$, is remarkably similar. From Figure 11 it can be seen that $\Delta g(r)$ for the asymmetric mixture is a somewhat longer range function leading to a slightly lower critical temperature as shown in Figure 10.

In Figure 12 we have plotted the structure factors for the same two mixtures depicted in Figure 11. For the symmetric isotope there is only one independent structure factor shown by the points. For the asymmetric mixture $\hat{S}_{AA}(k)$ and $\hat{S}_{BB}(k)$ are distinct at larger wave vector but both diverge at the critical point for $k = 0$. The lines refer to $\hat{S}_{RPA}(k)$ calculated from eqs 9 and 10 using the zero wave vector value for χ. It can be seen that the RPA calculation is exact at $k = 0$ for the symmetric blend, but is significantly in error for the asymmetric case. A positive intercept is expected for the RPA in the asymmetric blend

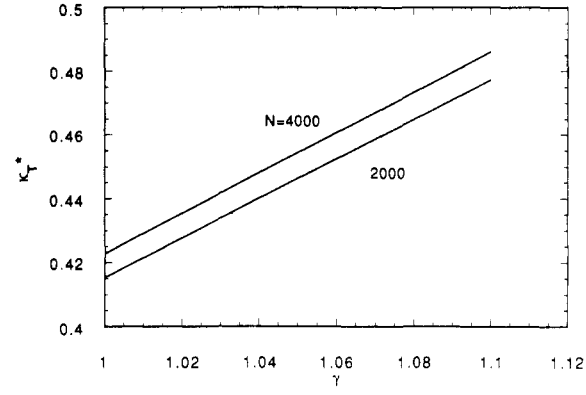

Figure 13. Reduced isothermal compressibility $\kappa_T^* = \kappa_T(k_BT/\sigma_A^3)$ as a function of the asymmetry ratio γ at $T^* = 273$ and $\eta = 0.45$ for two different chain lengths.

since $\hat{S}_{RPA}(0)$ is given by eq 21 with χ having a negative value. Even though the RPA is reasonably close to the exact calculations at high wave vector, it breaks down in the $k = 0$ thermodynamic limit. This result raises serious questions concerning the molecular meaning of the χ parameters determined by the common data analysis procedures (either $k = 0$ extrapolation or fitting the wave vector dependence to the RPA form).

Since the RPA is known to be exact in the incompressible limit ($\kappa_T = 0$), we calculated the isothermal compressibility from eq 14 as a function of the structural asymmetry γ. The dimensionless compressibility κ_T^* is plotted in Figure 13 at fixed temperature for two different chain lengths. It is interesting to note that κ_T^* is a linearly increasing function of γ. Since the compressibility of the $\gamma = 1.10$ asymmetric blend is only 13% greater than the symmetric case, we speculate that the compressibility of the model symmetric isotope blend would invalidate the RPA approximation were it not for the fact that composition and density fluctuations are rigorously independent[19,21,22] for the 50/50 mixture. Our general conclusion from the simple Gaussian model calculations presented here is that structural asymmetry greatly reduces the incompressible χ parameter, but this stabilization is largely (and possibly entirely) counterbalanced by the mixture-destabilizing consequences of spontaneous density fluctuations. Hence the actual net effect of structural asymmetries on T_c and phase stability is very subtle and an inherently sensitive function of nonuniversal, local structure. Therefore, in our opinion, definitive progress requires a chemically realistic treatment of molecular structure (e.g., stiffness, aspect ratio, range of nonbonded forces, etc.) at *constant* pressure, a theoretical program we intend to pursue in future studies. It should be mentioned that Dudowicz and Freed[34] have also recently studied compressible polymer mixtures using various lattice models with vacancies. These authors likewise concluded that the RPA approximation should be used with caution when applied to compressible blends and that local structural details can be of paramount importance.

From Figures 6 and 12 it can be seen that $[\hat{S}_{AA}(k)]^{-1}$ is approximately linear in k^2. This suggests that one could define a χ parameter operationally according to

$$\chi_{eff} \equiv \frac{1}{2}\left[\frac{1}{R^{1/2}\phi N_A} + \frac{R^{1/2}}{(1-\phi)N_B} - \frac{1}{\hat{S}_{AA}(0)}\right] \qquad (33)$$

by rearranging eq 21. Equation 33 is often employed by experimentalists in conjunction with *background subtraction procedures*. In a SANS experiment, the scattered intensity of a general binary blend is a linear combination of the three partial structure factors, weighted by the cor-

responding scattering cross sections. Therefore, in principle, two additional χ parameters, based similarly on $\hat{S}_{BB}(k)$ and $\hat{S}_{AB}(k)$, would also be necessary to fully describe the scattering intensity. Since three independent χ parameters are required to describe a general binary blend, the usefulness of this operational definition is questionable and one might as well employ the exact structure factors in eqs 7. In addition, definitions of χ such as in eq 33 can also lead to unphysical, divergent behavior of the inferred χ in one or both of the pure component limits.

The limitations of the RPA analysis discussed here were based on calculations for Gaussian chains. We have shown previously[15] that the compressibility of homopolymer liquids of Gaussian chains is significantly higher than for semiflexible chains which more faithfully represent the intramolecular structure of real polymer molecules and the resultant local interchain packing. Furthermore, all of the calculations shown here were for a packing fraction η of 0.45, which is somewhat low compared to real systems. Increasing the packing fraction to 0.50 or higher would also have the effect of further lowering the isothermal compressibility. Presumably a reduction in κ_T would lead to an improvement in the accuracy of the RPA approximation. Calculations are underway on blends of semiflexible chains in order to address the question of the quantitative usefulness of RPA-based analysis of SANS data in real systems.

In summary, our computations on Gaussian chain blends using our RISM-MSA integral equation methods have allowed us to draw several general conclusions regarding polymer blends:

(1) Perhaps the most provocative conclusion we draw is that the χ parameter should vary inversely with the square root of the molecular weight for both symmetric and weakly asymmetric blends. A corollary is that the UCST should increase with $\sqrt{N}$ rather than a linear molecular weight dependence predicted by Flory–Huggins theory. A rigorous experimental test of this surprising prediction has yet to be performed.

(2) Our results for the composition dependence of the χ parameter are in good qualitative agreement with the recent SANS experiments of Bates and collaborators[38] on isotopic polymer blends. In all cases we are able to correctly predict the qualitative trends reported by these authors.

(3) The RPA for the structure factor progressively deteriorates as the structural asymmetry increases. The limitations of the RPA approach found here are amplified for fully flexible, Gaussian chain mixtures.

Future calculations on blends will be performed employing more realistic representations of the intramolecular structure and interchain forces. Using $\hat{\omega}_A(k)$ and $\hat{\omega}_B(k)$ functions which include chain stiffness effects, we are currently investigating cases where the pressure, rather than the volume, is held fixed. We anticipate that such calculations may show evidence of compressibility induced LCST behavior. In the future we also plan to carry out intramolecular/intermolecular self-consistent calculations on blends to investigate concentration-dependent, nonideality effects on both local and global length scales. Finally, it should be mentioned that methods similar to those used here on blends can be applied to study the structure and thermodynamics of block copolymers and chains of other, more complex, topology.

References and Notes

(1) Wignall, G. D.; Bates, F. S. *MRS Bull.* **1990**, *15* (Nov), 73.
(2) Flory, P. J. *Principles of Polymer Chemistry*; Cornell University Press: Ithaca, NY, 1953.
(3) Bates, F. S.; Muthukumar, M.; Wignall, G. D.; Fetters, L. J. *J. Chem. Phys.* **1988**, *89*, 535.
(4) Ito, H.; Russell, T. P.; Wignall, G. D. *Macromolecules* **1987**, *20*, 2214.
(5) Trask, C. A.; Roland, C. M. *Macromolecules* **1989**, *22*, 256.
(6) Brereton, M. G.; Fischer, E. W.; Herkt-Maetzky, C.; Mortensen, K. *J. Chem. Phys.* **1987**, *87*, 6144.
(7) Schweizer, K. S.; Curro, J. G. *Phys. Rev. Lett.* **1987**, *58*, 246.
(8) Curro, J. G.; Schweizer, K. S. *Macromolecules* **1987**, *20*, 1928.
(9) Curro, J. G.; Schweizer, K. S. *J. Chem. Phys.* **1987**, *87*, 1842.
(10) Schweizer, K. S.; Curro, J. G. *Macromolecules* **1988**, *21*, 3070.
(11) Schweizer, K. S.; Curro, J. G. *Macromolecules* **1988**, *21*, 3082.
(12) Chandler, D.; Andersen, H. C. *J. Chem. Phys.* **1972**, *57*, 1930.
(13) Chandler, D. In *Studies in Statistical Mechanics*; Montroll, E. W., Lebowitz, J. L., Eds.; North-Holland: Amsterdam, 1982; Vol. VIII, p 274, and references cited therein. Chandler, D. *Chem. Phys. Lett.* **1987**, *140*, 108.
(14) Curro, J. G.; Schweizer, K. S.; Grest, G. S.; Kremer, K. *J. Chem. Phys.* **1989**, *91*, 1357.
(15) Honnell, K. G.; Curro, J. G.; Schweizer, K. S. *Macromolecules* **1990**, *23*, 3496.
(16) Honnell, K. G.; McCoy, J. D.; Curro, J. G.; Schweizer, K. S.; Narten, A.; Habenschuss, A. *J. Chem. Phys.* **1991**, *94*, 4659.
(17) Schweizer, K. S.; Curro, J. G. *Phys. Rev. Lett.* **1988**, *60*, 809.
(18) Curro, J. G.; Schweizer, K. S. *J. Chem. Phys.* **1988**, *88*, 7242.
(19) Schweizer, K. S.; Curro, J. G. *J. Chem. Phys.* **1989**, *91*, 5059.
(20) Curro, J. G.; Schweizer, K. S. *Macromolecules* **1990**, *23*, 1402.
(21) Schweizer, K. S.; Curro, J. G. *Chem. Phys.* **1990**, *149*, 105.
(22) Schweizer, K. S.; Curro, J. G. *J. Chem. Phys.* **1991**, *94*, 3986.
(23) de Gennes, P. G. *Scaling Concepts in Polymer Physics*; Cornell University Press: Ithaca, NY, 1979. Leibler, L. *Macromolecules* **1980**, *13*, 1602.
(24) Schweizer, K. S.; Honnell, K. G.; Curro, J. G. *J. Chem. Phys.*, submitted.
(25) Flory, P. J. *J. Chem. Phys.* **1949**, *17*, 203.
(26) Lowden, L. J.; Chandler, D. *J. Chem. Phys.* **1974**, *61*, 5228; **1973**, *59*, 6587; **1975**, *62*, 4246.
(27) Hansen, J. P.; McDonald, I. R. *Theory of Simple Liquids*; Academic Press: London, 1986.
(28) Honnell, K. G.; Hall, C. K.; Dickman, R. *J. Chem. Phys.* **1987**, *87*, 664.
(29) Gao, J., Weiner, J. H. *J. Chem. Phys.* **1989**, *91*, 3168.
(30) Schweizer, K. S., Curro, J. G. *J. Chem. Phys.* **1988**, *89*, 3342.
(31) Kirkwood, J. G.; Buff, F. P. *J. Chem. Phys.* **1951**, *19*, 774.
(32) In ref 19 the authors incorrectly stated in eq 2.22 that the isothermal compressibility was proportional to a linear combination of partial structure factors at zero wave vector.
(33) Sanchez, I. C. *Macromolecules* **1991**, *24*, 908.
(34) Dudowicz, J.; Freed, K. F. *Macromolecules* **1990**, *23*, 1519. Tang, H.; Freed, K. F. *Macromolecules* **1991**, *24*, 958.
(35) Sariban, A.; Binder, K.; Heermann, D. W. *Phys. Rev. B* **1987**, *35*, 6873. Sariban, A.; Binder, K. *J. Chem. Phys.* **1987**, *86*, 5859.
(36) Brereton, M. G.; Fischer, E. W.; Herkt-Maetzky, C.; Mortensen, K. *J. Chem. Phys.* **1987**, *87*, 6144.
(37) Bates, F. S.; Wignall, G. D.; Koehler, W. C. *Phys. Rev. Lett.* **1985**, *55*, 2425. Bates, F. S.; Wignall, G. D. *Phys. Rev. Lett.* **1986**, *57*, 1429.
(38) Bates, F. S.; Muthukumar, M.; Wignall, G. D.; Fetters, L. J. *J. Chem. Phys.* **1988**, *89*, 535.
(39) Jung, W. G.; Fischer, E. W. *Makromol. Chem., Makromol. Symp.* **1988**, *16*, 281.
(40) Malescio, G. *Phys. Rev. A* **1990**, *42*, 2211, 6241.
(41) Almdal, K.; Rosedale, J.; Bates, F. S.; Wignall, G. D.; Fredrickson, G. H. *Phys. Rev. Lett.* **1990**, *65*, 1112.
(42) Freid, H.; Binder, K. *J. Chem. Phys.* **1991**, *94*, 8349.